

# THE PROCESSING OF HELICAL-WELDED LARGE DIAMETER PIPES OF GRADE X80 WITH 23.7 mm WALL THICKNESS AND THEIR PROPERTIES

Franz Martin Knoop<sup>2</sup> Sandrine Bremer<sup>1</sup>, Volker Flaxa<sup>1</sup>, Wolfgang Scheller<sup>1</sup> and Markus Liedtke<sup>1</sup>

<sup>1</sup>Salzgitter Mannesmann Forschung GmbH, Germany

<sup>2</sup>Salzgitter Mannesmann Großrohr GmbH, Germany

Keywords: API X80, Niobium, Hot-coiled Strip, HTP, SAWH-pipe, Bainite, Weldability, HAZ

## Abstract

In recent years the development of large diameter, thick wall helical-welded linepipe grade API X80 was a priority. Hot-coiled strips, spiral pipes and submerged arc welds have been produced and microstructure, texture and mechanical properties have been characterized. Good field weldability was proven. The favourable microstructure has been achieved by the selection of an appropriate chemical composition of low carbon content and an increased amount of niobium in combination with a thermo-mechanical hot rolling process. The addition of niobium in combination with the adjustment of other alloying elements allowed improved slab reheating conditions and increased the recrystallisation stop temperature (high temperature processing: HTP). A homogeneous microstructure across the strip gauge was formed during accelerated cooling on the run-out table of the hot rolling mill. All results met the requirements for API X80 pipes which were determined for a wall thickness of 23.7 mm x OD 813 mm and 23.7 mm x OD 1220 mm. The bainitic microstructure and mechanical properties of the pipe base material and welding zones are discussed.

## Introduction

Within the last decade, the usage of X80 pipes for high-pressure gas pipelines has changed from test series to real alternatives for long pipelines. While at the beginning of the nineties, the first X80 pipelines were exclusively produced with steel plates and SAW longitudinal-welded pipes, the acceptance to use spiral-welded pipes of grade X80 is now growing all over the world. The significant cost for construction of natural gas pipelines is one of the main drivers for maintaining the competitiveness of gas compared to alternative energy sources. The development of high strength steels for large diameter linepipe is pushed by the need to reduce these costs [1].

The production of high strength, thick-walled hot-coiled strip and spiral pipes is a challenge and plant equipment has to bear high forces; for example finish rolling mill, down-coiler, re-coiler, levelling machine and pipe forming machine.

## Processing of Steel and Hot-Rolled Strips

To start with, lab-scale trials with different chemical compositions for grade X80 were produced and hot-rolled to evaluate different temperature settings and find the optimised conditions for the hot-rolling mill. The second and third steps were steel making and hot rolling on an industrial scale. The first coils from which spiral pipes with different dimensions were produced, had a thickness of 14.1 mm [2] followed by 18.9 mm [3-6] and 23.7 mm. The actual chemical composition for grade X80 with a wall thickness of 23.7 mm is given in Table I.

Table I. Chemical Composition of Salzgitter`s API X80 23.7 mm [wt %]

Steel	C	Si	Mn	Al	Ti	Nb	$\Sigma$ Cu, Cr, Ni, Mo
X80 (t >20 mm)	0.05	0.30	1.9	0.05	0.01	0.09	< 0.40

Salzgitter is an integrated steel works which provides the possibility to adapt metallurgical processing for special grades such as API X80. After tapping from the blast furnace and de-sulphurisation of the pig iron, oxygen blowing in the LD-converter is applied and followed by micro-alloying in the secondary metallurgy. Continuous casting is carried out with the use of dynamic soft reduction.

Subsequently the slabs are delivered to the re-heating furnaces of the hot strip mill. A time-temperature-controlled re-heating process combined with the low carbon content leads to a homogeneous dissolution of carbides and provides uncontrolled grain growth. The dissolution of Nb (C,N) during reheating is additionally ensured by an appropriate holding time to take advantage of Nb-precipitation hardening contribution later on. In this way, the requirements are met for assuring high yield strength and very good toughness properties of the pipe material. Figure 1 shows a numerical calculation of slab re-heating temperature (SRT) as a function of niobium content to ensure niobium dissolution. All other amounts of elements correspond to Table I.

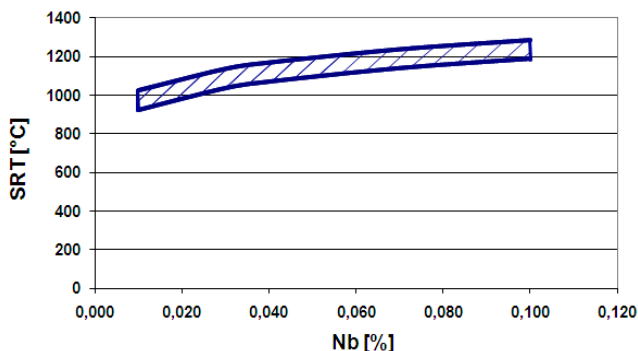


Figure 1. Slab re-heating temperature (SRT) range vs. niobium content, calculated for chemical composition given in Table I, to dissolve Nb (C,N).

Adding certain amounts of niobium and reducing the carbon content leads to an increase of the recrystallisation stop temperature. Thus, higher rolling temperatures allow higher reduction rates in the area of non-recrystallised austenite. By applying higher reduction rates, a large number of nucleation sites are introduced into the material and the  $\gamma$ - $\alpha$  (Austenite to Ferrite) transformation results in a fine grained ferrite or an even bainitic microstructure. Immediately after finish rolling, the final cooling of the material is carried out which is of great importance before the coil cools down slowly after down-coiling. A Time-Temperature-Transformation diagram is shown in Figure 2, and a schematic HSM cooling rate added for the mid-thickness of the strip/pipe. The applied cooling rate leads to a predominantly bainitic microstructure with small portions of ferrite, Figure 3.

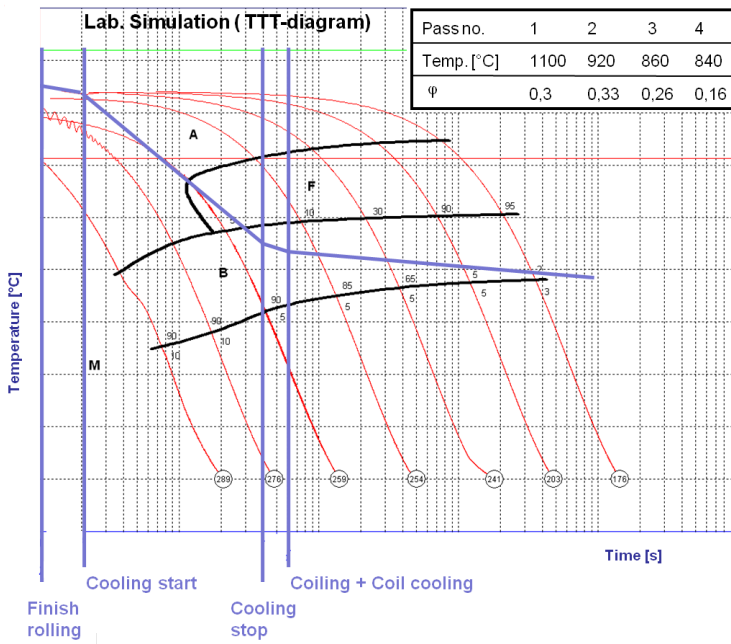


Figure 2. Transformation of microstructure during accelerated cooling after deformation (logarithmic true strain  $\varphi$ ) simulation: Lab trials (TTT-diagram) and schematic HSM cooling rate (blue curve).

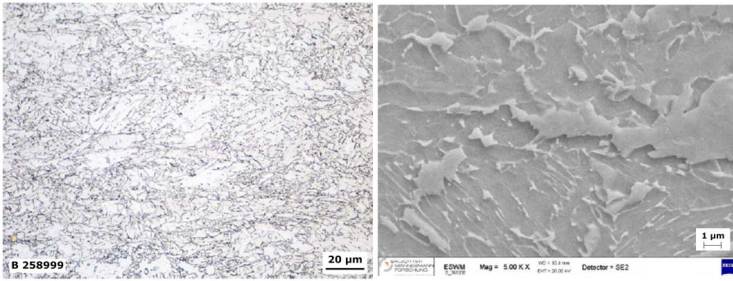


Figure 3. Microstructure of API X80,  $t=23.7$ mm, mid-thickness (Nital).

- a) Light optical microscope (LOM).      b) Scanning electron microscope (SEM).

### Correlation between Mechanical Properties, Microstructure and Rolling Texture in Coil

Because of residual stresses in the bainitic sub-grained microstructure of X80 hot-coiled strips, a lot of dislocations are present which are indicated by round-house stress-strain curves during tensile testing. These stress-strain curves, Figure 4, are characterised by a continuous and steady change from elastic into plastic yielding without any Lüders elongation. The different angles ( $0^\circ$ ,  $23^\circ$ ,  $67^\circ$ ,  $90^\circ$ ) to the rolling direction have no effect on the round-house shape of the stress-strain curves for the investigated samples. Hot-coiled strip data presented in this section corresponds to angles of  $23^\circ$  and  $67^\circ$  (see Table II, OD 1220 mm).

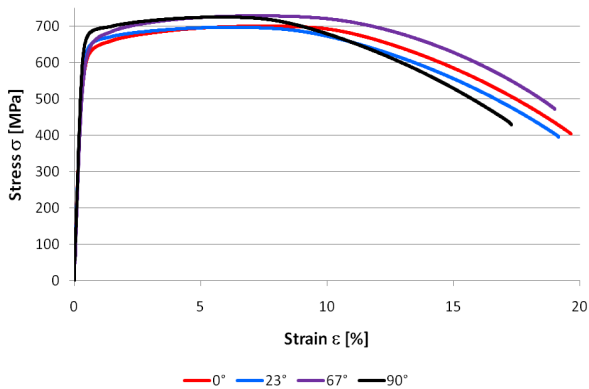


Figure 4. Stress-strain curves for full section hot-coiled strip samples at different angles to rolling direction, (23.7 mm wall thickness).

For hot-coiled strips with  $t=23.7$  mm, mechanical properties were evaluated by tensile testing at different angles to the rolling direction, Figure 5.

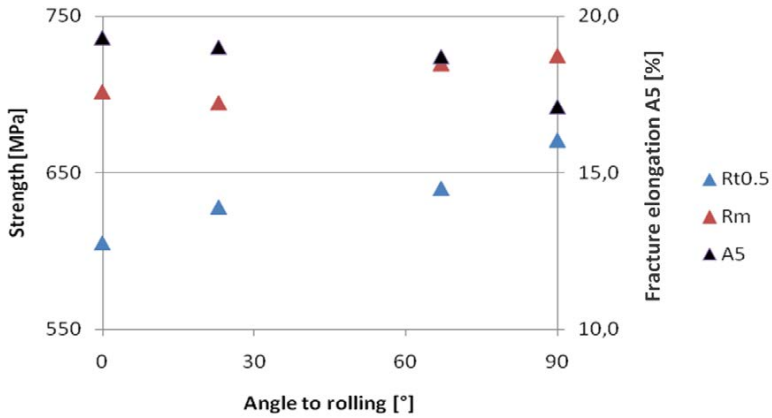


Figure 5. Mechanical properties of hot-coiled strip after tensile testing at different angles to rolling direction, full section samples, wall thickness of 23.7 mm.

Yield ( $R_{t0.5}$ ) and tensile strength ( $R_m$ ) for the longitudinal ( $0^\circ$  to rolling) and hoop directions ( $23^\circ$  to rolling) are slightly lower than for the pipe axis ( $67^\circ$  to rolling) and transverse directions ( $90^\circ$  to rolling). The fracture elongation in turn decreases with increasing strength from 19.3% ( $0^\circ$  to rolling) to 17.1% ( $90^\circ$  to rolling).

In order to identify a correlation between mechanical properties of tensile testing and the material's microstructure, the rolling texture was evaluated by electron back-scatter diffraction (EBSD), Figure 6. From the orientation data obtained by EBSD, orientation distribution functions (ODF) were calculated.

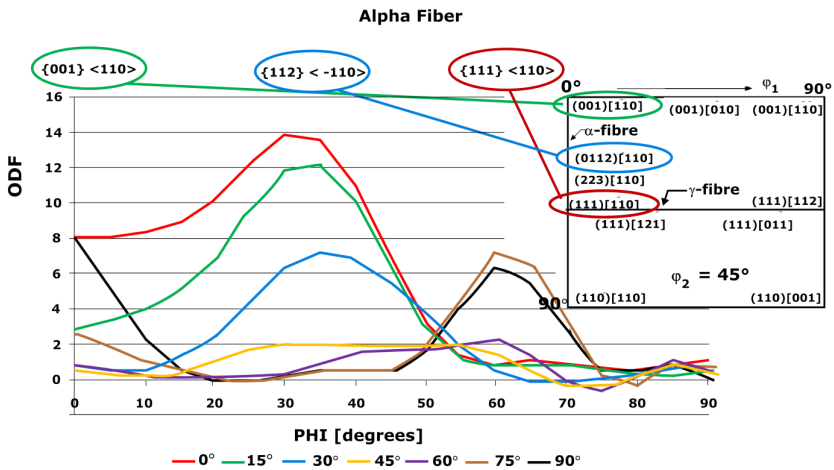


Figure 6. ODF  $\phi=45^\circ$  section: X80 texture evaluation of hot-coiled strip for different angles to rolling direction, mid-thickness; small graph: ideal orientations for bcc-materials.

$\phi$ -direction equals the sample's rolling direction. The rolling directions ( $0^\circ$ ) shows major texture components for  $\{112\}\langle 110\rangle$  ( $\{\dots\}$ planes and  $\langle\dots\rangle$  direction). While evaluating the angles to rolling direction and moving to transverse ( $90^\circ$ ) direction by  $15^\circ$  steps, this major component fades and a new major texture component  $\{111\}\langle 110\rangle$  appears. According to literature [7],  $\{111\}\langle 110\rangle$  components are responsible for higher material strength which may be the reason for the higher yield strength in  $67^\circ$  (pipe axis) and  $90^\circ$  (transverse to rolling) compared to rolling direction, Figure 5.

### Pipe Production

Pipes with OD of 813 and 1220 mm and a wall thickness of 23.7 mm have been produced by Salzgitter Mannesmann Grobrohr GmbH using the Helical Two Step-Technology (HTS) [8]. The process is split into pipe forming combined with continuous tack-welding and final internal and external submerged arc welding at separate welding stations, Figure 7. By separating the forming from the welding process each step can be optimized in terms of quality and process efficiency. Pipe forming and tack welding up to 15 m/min is achieved.

## Helical Seam Two Step -Process

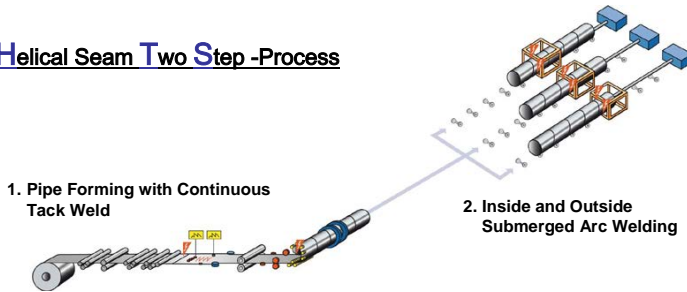


Figure 7. HTS Process.

The forming process (**step one**) consists of three sections:

- Uncoiling of hot-rolled 1500 mm wide strips
- Levelling in a multi-roller levelling unit
- Forming the coil into a pipe at a forming angle  $\alpha$ .

The hot-rolled wide strip is formed into a pipe in the pipe-forming machine. This forming unit consists of a three-roll bending system with an outside roller cage. The converging strip edges of the pipe are joined with a continuously shielded arc tack weld. As the continuously-tack-welded pipe leaves the forming machine, a plasma cutter, moving with the tube, cuts the individual lengths required by the customer. Tack welding is done automatically and by means of a laser-guided welding head. To optimise the pipe and weld gap geometry, the run-out angle is also permanently controlled and adjusted by an automatic gap control system. Any changes in the coil width because of variations in the coil dimensions before or after milling do not affect the final pipe geometry. This forming angle can be calculated according to the following equation using the pipe diameter ( $D$ ) and the width ( $B$ ) of the hot-rolled coil. Finite element modelling has been used to optimise the influence of the levelling process and the pipe forming and to achieve a minimised spring back of the formed pipe [4]. To realise perfect pipe geometry with the smallest possible tolerances on diameter and ovality a newly designed and patented automatic in-line diameter process control system was also used [9].

$$\alpha = \arcsin\left(\frac{B}{\pi \cdot D}\right) \quad (1)$$

By using Equation (1), pipe forming angles  $\alpha$  of  $23^\circ$  for 1220 mm OD and  $36^\circ$  for 813 mm OD can be calculated. The pipe hoop and longitudinal direction are placed  $23^\circ$  (pipe hoop) and  $67^\circ$  (pipe axis) for OD 1220 mm and  $36^\circ$  (pipe hoop) and  $54^\circ$  (pipe axis) for OD 813 mm to the rolling direction of the coil material, Table II, Figure 8.

Table II. Angles to Rolling Direction and Orientation at Pipes

angle to rolling direction [°]	position at spiral pipe for strip width 1,500 mm
0	parallel to SAW
23	Hoop (OD 1220 mm)
36	Hoop (OD 813 mm)
(-)54	Pipe axis (OD 813 mm)
(-)67	Pipe axis (OD 1220 mm)
90	Perpendicular to SAW

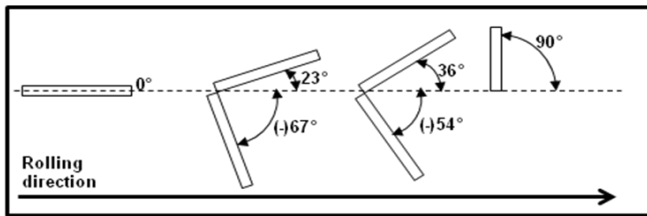


Figure 8. Schematic illustration of angle to rolling direction.

In the **second process step**, the formed and continuously-tack-welded pipes are then subsequently fed into one of the three computer-controlled, internal/external submerged-arc welding stations for final welding. Each pipe rotates on a special roller table with a precise screw-like motion while submerged-arc welding is carried out, first internally, then externally, with a multi-wire technique. A laser-controlled seam tracking system guarantees exact positioning of the weld seam with optimised overlapping and penetration of the weld. The tack weld made during the pipe-forming stage serves as a backing for the weld and is fully melted again.

### Mechanical Properties of Pipe Base Material

When forming the hot-coiled strip into spiral pipes for the given angles, 23° or 36°, the dislocation density is increased and a strain hardening effect is evident especially for the hoop direction of the pipes. This strain hardening effect depends on the diameter to wall thickness ratio ( $D/t$ -ratio). In Figure 9, yield and tensile strength ( $YS/R_{0.5}$ ,  $UTS/R_m$ ) of flattened full section samples and round bar samples before and after ageing are compared for both diameters.

For the hoop direction of OD 813 mm, the sample geometry seems to have an influence on the pipe yield strength. Full section samples are flattened before testing. This additional cold deformation may lead to an increase of dislocations in an already distorted base material and thus, yield strength can be increased. For round bar specimens, flattening is not applied for high wall thicknesses. After ageing, samples from the hoop direction show an increase in yield strength which may be caused by free nitrogen (bake-hardening effect) in combination with the high deformation. The pipe axis in turn is not exposed to the deformation and thus, no difference before and after ageing appears. Tensile strength is not affected by flattening [10].

For the hoop direction in OD 1220 mm pipes, the same conclusion can be drawn for yield and tensile strength as well as for fracture elongation. The difference between flattened full section samples and round bar samples is somewhat smaller than for OD 813 mm. The D/t-ratio is greater for pipes with OD 1220 mm, therefore less cold deformation is applied to the material during pipe forming and less deformation is needed for sample flattening.

A comparison of hoop and pipe axis shows a difference in yield strength from hoop to pipe axis of 60 MPa. The higher yield strength in the longitudinal direction and the additional stiffening effect of the spiral weld leads to a higher resistance to plastic deformation in the longitudinal direction compared to the circumferential direction.

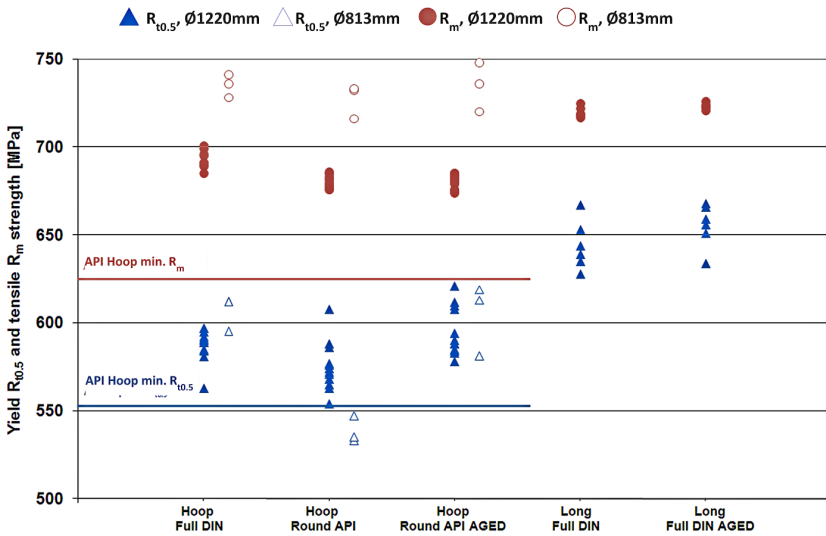


Figure 9. Yield and tensile strength determined for hoop direction and pipe axis direction on different sample geometries after pipe forming and after pipe coating (ageing at 200 °C).

In Figure 10 fracture elongation and Y/T-ratio ( $A_{DIN}$ ,  $A_{API}$ ,  $R_{10.5}/R_m$ ) of flattened full section samples and round bar samples before and after ageing are compared for both diameters. Y/T-ratio for both diameters and all sample types is lower than the API-limit of 0.93. Fracture elongation strongly depends on the sample geometry, especially the gauge length  $L_0$  which is  $L_{0, DIN}=140$  mm and  $L_{0, API}=50.8$  mm.

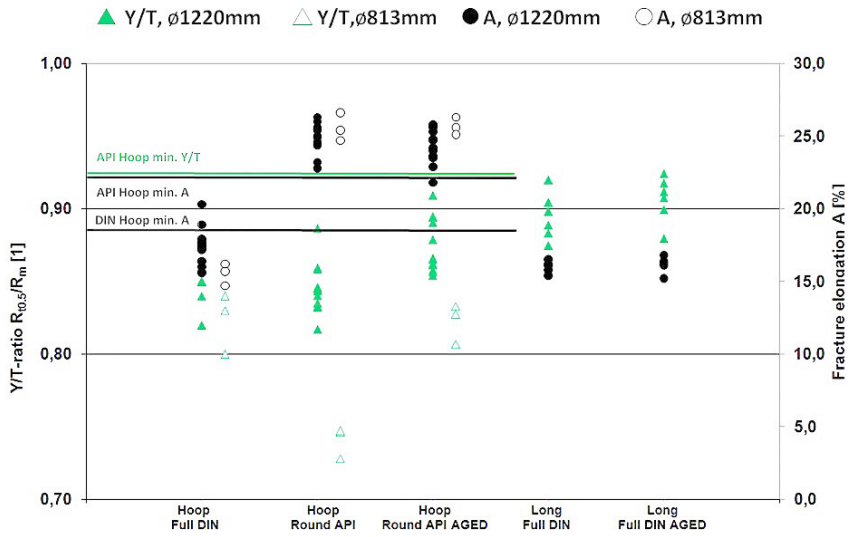


Figure 10. Fracture elongation and Y/T-ratio for hoop direction and pipe axis on different sample geometries after pipe forming and after pipe coating (ageing at 200 °C).

To fully characterise mechanical properties, low-temperature toughness was investigated for the pipe material by testing Charpy V-notched samples, Figure 11. The low carbon content and the higher niobium level also led to high upper shelf toughness values with small standard deviations.

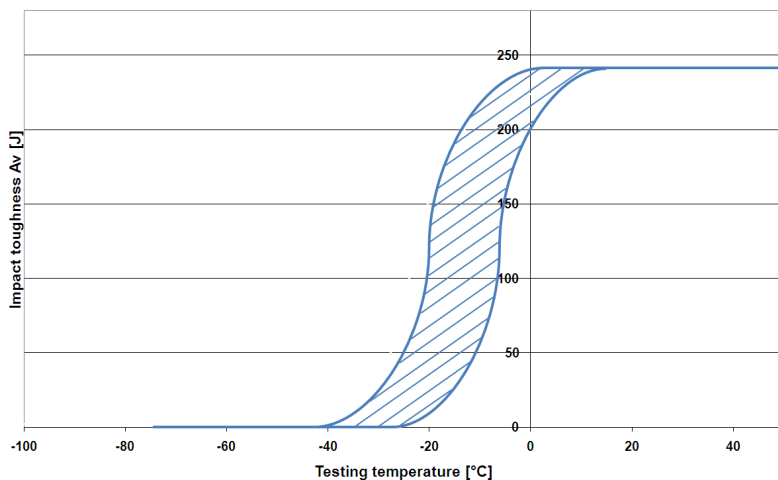


Figure 11. Transition area for Charpy V-notched samples for OD 813 mm and OD 1220 mm, hoop direction of pipes.

Shear fracture appearance after drop weight tear testing was also evaluated on several pipes of OD 1220 mm. At a testing temperature of 0 °C, the samples shear area was determined as 85 to 100%.

### Weldability Assessment

Generally, the welding conditions for higher strength X80 linepipes are more restricted and challenging in order to satisfy the requirements compared to lower strength grades. The micro alloy design and compositional control of these TMCP (Thermo-Mechanically Controlled Processed) steels is more critical in order to achieve the desired properties, such as satisfactory weld metal and HAZ toughness and suitable field weldability, in order to avoid problems such as cold cracking in the heat affected zone. Welding procedure variables such as pre-heat, interpass temperatures and overall welding parameters are much more stringent and must be carefully controlled and monitored. Nevertheless, the consumables used to weld X80 base material must meet the material's strength requirements providing good toughness properties at the same time. With regard to strain-based design demands, weld joints in pipelines also require strength overmatching, because a higher strain to failure is obtained for overmatched welded joints compared to undermatched welded joints [11-13].

Furthermore, a major concern for higher strength steels is also the cold cracking susceptibility in the HAZ due to the alloying concepts and resulting higher carbon equivalents. The occurrence of cold cracking is linked to three factors: diffusible hydrogen content in the weld metal, brittle microstructure, and residual stresses. Diffusible hydrogen comes mainly from the filler material and from atmospheric conditions. The brittleness of the microstructure is linked to the chemical

composition of the weld metal and of the base metal and to the thermal cycle during welding [12, 13].

### Thermal Cycle Simulation

Before starting X80 Helical Two Step (HTS) pipe production by Salzgitter Mannesmann Großrohr GmbH (MGR), numerous test series of thermal cycle simulations and cold cracking tests were performed in advance on the strip base material to simulate the effect of different welding conditions (production and field welding) in order to get fundamental information of the corresponding HAZ characteristics and properties.

Thermal cycle simulations were performed to simulate the coarse grain heat affected zones (CGHAZ) generated by typical welding cooling times ( $t_{8/5}$ ) of welding techniques such as GMAW (field welding) and SAW (HTS pipe production). The combination of microstructural constituents formed in any HAZ region is mainly a function of the chemical composition of the steel and the weld cooling rate. Simulations of this HAZ region, which is often associated with low toughness properties, can be performed in a single thermal cycle by heating up to a peak temperature (typical holding time of 1 s) and cooling down to ambient temperature with the necessary time cycles. The distinctive temperature-time cycle during welding is expressed by cooling time  $t_{8/5}$ . During welding, time  $t_{8/5}$  is used to characterise the temperature-time cycle of an individual weld bead and is the time taken for a weld run and its HAZ to pass, during cooling, through a temperature range from 800 °C to 500 °C. This definition of the temperature time cycle is shown in Figure 12 [14,15].

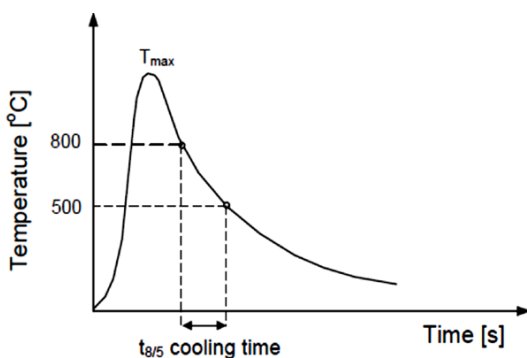


Figure 12. Typical temperature-time cycle and definition of cooling time  $t_{8/5}$  [14].

HAZ simulation tests were performed by a thermal cycle simulator, Figure 13, on specimens with a cross section 10.5 mm x 10.5 mm extracted transverse to the rolling direction of the X80 strip material. After heating to the peak temperature of 1200 °C – 1300 °C, this temperature was held for 1 second before controlled cooling was carried out with  $t_{8/5}$  times of 5 s, 10 s, 20 s and

40 s. These typical cooling times were used to investigate the CGHAZs in detail in terms of microstructure (light optical microscopy LOM), hardness and CVN (Charpy V-notch) testing.

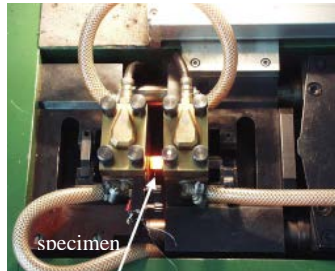


Figure 13. Thermal cycle simulator with mounted specimen during thermal treatment.

Quantitative microstructure analyses of the simulated CGHAZ by LOM revealed a bainitic microstructure with some proportion of martensite at fast cooling times between 5 s and 10 s (typical range for girth welding). This microstructure changed to predominantly bainite with longer cooling times in the range of 20 s and 40 s (production welds). The simulated CGHAZ microstructures are shown in Figure 14 for the lowest and highest  $t_{8/5}$  time respectively.

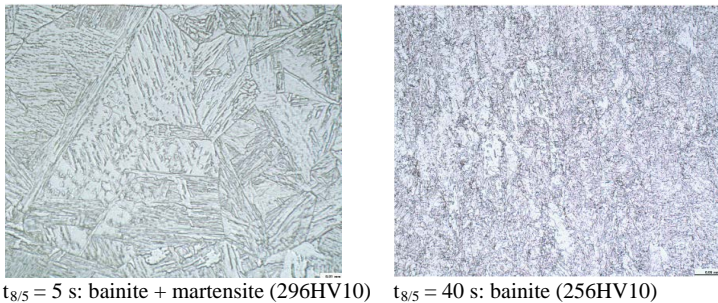


Figure 14. HAZ microstructure in thermal simulated specimens,  $t_{8/5} = 5$  s and 40 s (Nital).

The results of CVN testing at mild temperatures (0 °C) and hardness testing of the simulated HAZ specimens are summarised in Figure 15. As expected from the metallographic evaluation of the simulated specimens, the peak hardness decreases with increasing cooling time  $t_{8/5}$ . CVN specimens show a constant high value up to cooling times of 20 s.

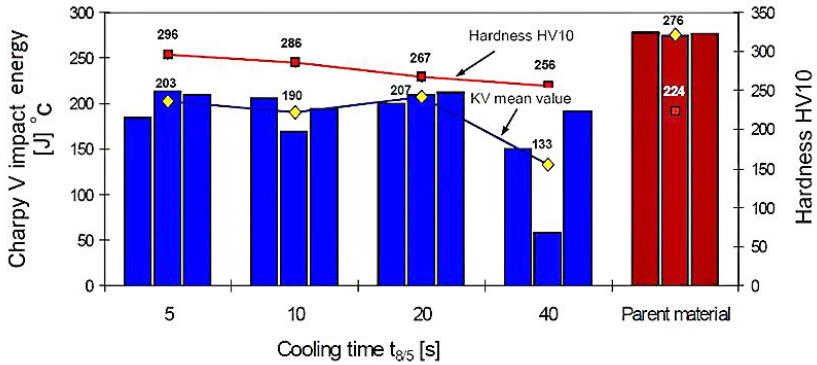


Figure 15. Impact energy and hardness of X80 simulated HAZ specimens.

In addition to these initial base material characterisations, the cold cracking susceptibility of this X80 hot strip material was also investigated by Tekken tests. Extensive Tekken tests performed according to EN ISO 17642-2 standard exhibited good material behaviour and insensitivity to cold cracking. Even for welding conditions where no pre-heating was applied (ambient temperature, 20 °C) no cracks were metallographically observed in the HAZ.

### Pipe Production and Welding

Due to the promising test results obtained for the base material in the pre-investigation test programme, trial production of X80 pipes was started using the Helical Two Step-Technology in order to investigate the corresponding properties (pipe base material and weld zones) in pipe. A submerged arc welding process with a multiple head arrangement was used with three welding heads inside, and three welding heads outside. EN 756 S1 and SZ wires in combination with rutile-acid and semi-basic flux were selected to achieve a moderate hardness increase in the final weld. Figure 16 shows a smooth weld bead profile, good slag release and no undercuts or weld defects. To enable a high level of productivity and welding speed a flux with high current carrying capacity was chosen, Table III.

Table III. Welding Parameters and Details for SAW

steel grade	X80
wall thickness	23.7 mm
welding process	GMAW and SAW
welding set up	3 wires inside and 3 wires outside
bevel preparation	root face 10 mm, bevel angle: 2 x 40°, inside-V: 11 mm, outside -V: 11 mm
welding wires	EN 756 S1 and EN 756 SZ (3 to 4 mm)
welding flux	Inside: EN 760 SA CS 1 77 AC H5 (rutile-acid agglomerated calcium-silicate type flux) Outside: EN 760 FB 1 67 AC H5 (semi basic agglomerated fluoride – basic type flux)
welding speed	1.3 m/min
welding parameters (V +/- 10%; A +/- 15%)	33 to 35 V inside and 31 to 32 V outside 600 to 950 A inside and 650 to 1200 A outside
energy input	6 kJ/mm
preheating	None

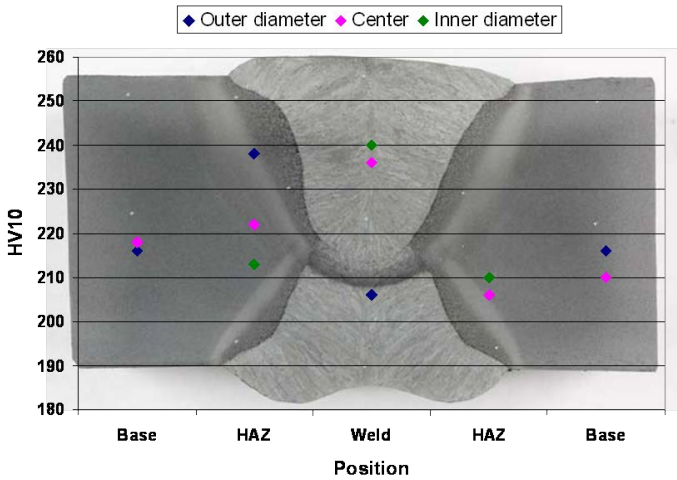


Figure 16. Hardness indentions HV10 and weld micrograph (Light optical microscope, Nital), wall thickness 23.7 mm.

Bending trials have been carried out for an angle of 180° with a bending radius of 6xt without cracking. The average tensile strength of the submerged arc weld was 736 MPa with a failure

position in the weld material. Low temperature toughness has been evaluated with Charpy V-notched samples for weld metal and heat affected zone before and after ageing at 200 °C, Figure 17.

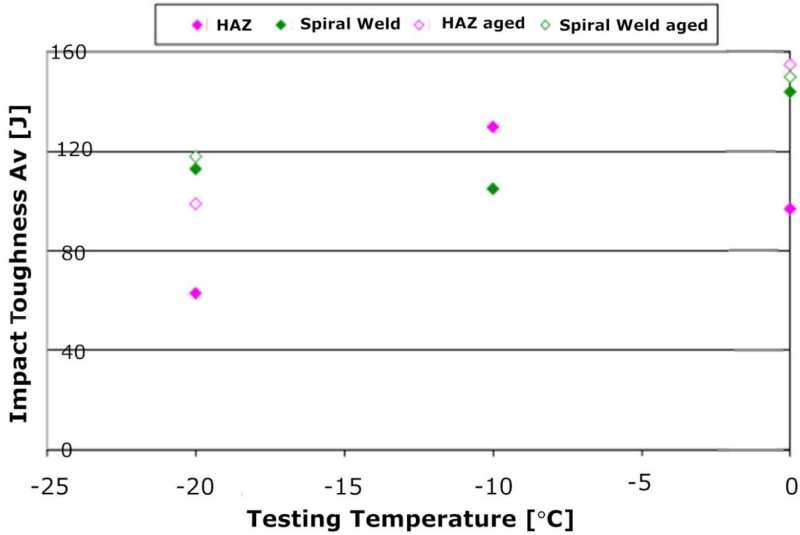


Figure 17. Impact toughness for different testing temperatures in spiral weld and HAZ before and after ageing (200 °C), w.th. 23.7 mm.

Weld metal and heat affected zone meet the API requirements for a testing temperature of 0 °C. Ageing seems to have a positive influence especially on the HAZ properties which are increased by 40 J. During ageing (for example during coating or submerged arc welding), lattice distortion may be reduced and hard phases like martensite may be annealed and softened.

### Field Weldability

After successful production of helical line X80 pipes with a wall thickness of 23.7 mm, field welding trials were performed by Salzgitter Mannesmann Forschung in Duisburg. These welding trials were carried out in order to investigate the mechanical and technological properties in the weld metal and in the heat affected zone of the base material. The lab welds were performed with the GMAW process in the 1G position, Figure 18, using a typical narrow gap bevel preparation.



Figure 18. Weldability assessment of X80 HTS pipe segments (GMAW - 1G position).

The bevel preparations of the pipe segments and an example girth weld macrograph are given in Figure 19.

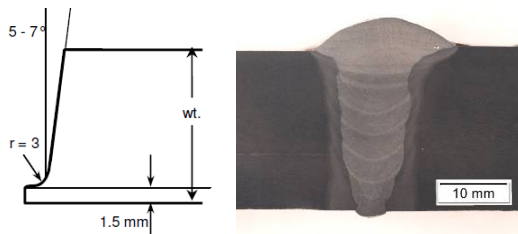


Figure 19. Pipe bevel preparation and corresponding girth weld macrograph.

Root pass welding was carried out using a solid wire of AWS type ER70S-G and shielding gas C1 (100% CO<sub>2</sub>). The remaining filler and cap passes were welded with a solid wire of AWS type ER90S-G and shielding gas M21 (82% Ar and 18% CO<sub>2</sub>). Before welding, the pipe segments were pre-heated up to 100 °C and a maximum interpass temperature of ca. 140 °C was maintained during the individual weld runs. The heat input was limited for the individual passes below 1.0 kJ/mm (cooling time  $t_{8/5}$  around 6 s). The girth weld on the test pipe segment was tested by NDT techniques and evaluated by different destructive testing methods, e.g. according to API 1104 20<sup>th</sup> Edition standard. Cross-weld tensile, bend and further tests such as hardness and Charpy impact were carried out as well as metallographic examinations of the HAZ areas. With regard to the need for certain strength overmatching of girth weld metals, all-weld metal tensile test specimens were additionally taken out of the weld seam in the area of the cap and root region. The tensile test results (both cross- and all-weld) are summarised in Table IV.

Table IV. Results from Cross-Weld and All-Weld Metal Tensile Tests

cross-weld tensile test specimens *		all-weld metal tensile test specimens		
	Rm [MPa]		R <sub>10.5</sub> [MPa]	Rm [MPa]
with reinforcement	784-790	cap area	733-734	771-789
without reinforcement	715-720	root area	719-734	771-792

\* Fracture position consistently located in pipe base material.

As can be seen in Table IV, the girth weld provided a safe strength overmatching exceeding the specified minimum yield stress (SMYS) of 552 MPa and tensile strength (SMTS) of 621 MPa of the X80 base material. In addition to the weld metal strength properties, girth weld joints must also have a good deformation capability and a good resistance to failure under bending deformation. In accordance with the API 1104 specification, side-bend test specimens were extracted out of the girth weld joint and tested. No cracks were observed on the bent specimen surfaces.

Figure 20 shows the result of the hardness survey, performed on a macro slice extracted from the girth weld, in different areas of the base material, HAZ and weld metal. The maximum hardness value of 264 HV10 was measured in the weld metal cap area. The CVN transition curves measured at different positions (weld metal, fusion line and fusion line +2 mm) between 0 and -30°C are shown in Figure 21.

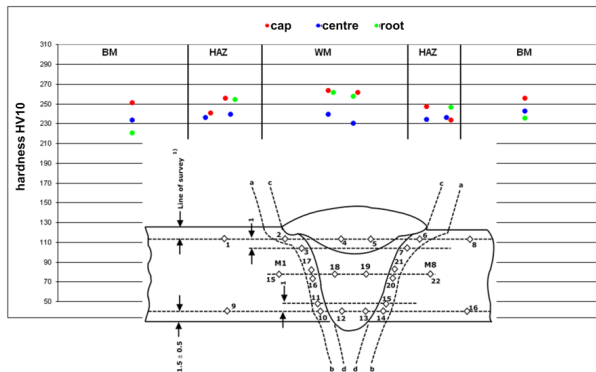


Figure 20. Hardness test results of X80 girth weld.

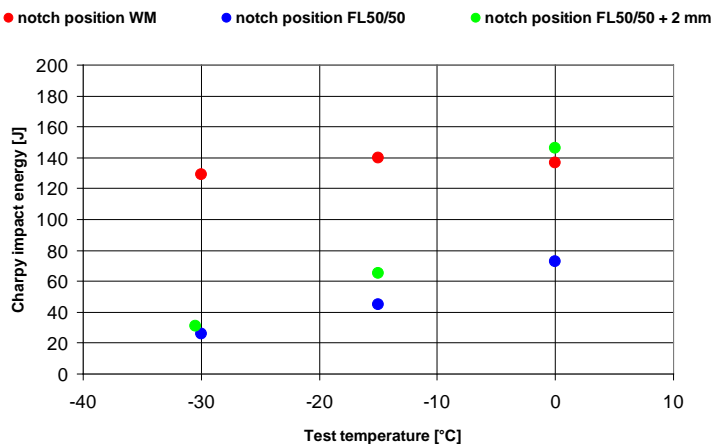


Figure 21. CVN test results of X80 girth weld.

Summarising the obtained test results of the performed welding trials it can be stated that this activity has confirmed the good overall weldability of X80 HTS pipes using GMAW techniques. On the basis of the API 1104 standard all test specimens achieved the requirements.

### Conclusions

To follow the market demands for increasing operating pressures and cost & energy efficiency, API X80 in 23.7 mm wall thickness has been developed, containing low carbon and higher niobium contents. The challenge of exposing plant equipment to high loads has been managed successfully. Spiral pipes with outer diameter of OD 1220 mm and OD 813 mm have been produced. The microstructure is predominantly bainitic. Mechanical properties of pipe manufactured met API requirements without any exception.

Intense welding investigations performed on X80 base and pipe material have confirmed good overall weldability for this steel grade using GMAW techniques. The welding consumables and conditions used (heat input, temperature control etc.) provided strength overmatching for the specified minimum yield stress and specified minimum tensile strength and also adequate toughness values down to a test temperature of -30 °C with mean values around 130 J. On the basis of the API 1104 standard all test specimens extracted from the girth weld fulfilled the requirements.

An optimisation in terms of low-temperature toughness is in progress and industrial trials will be carried out up to 25.4 mm wall thickness. The given steel chemistry with its niobium level of 0.09% is within the basic requirements of API5L and ISO 3138 but for specific projects end users inevitably call up various Annex requirements of these specifications which at the X80 strength level will typically limit niobium to 0.08% for low carbon offshore pipe or pipe intended

for sour service, and 0.07% for any onshore European gas transmission pipeline. Equally EN 10208-2 limits the maximum niobium content to 0.06%, therefore as an increased use of X80 pipe in European pipeline networks is expected, the current limits need to be revised because of economic and technical reasons. All results in this development work prove the positive effect of using niobium in high grade steels for line pipe applications.

## References

1. P. Bilston and M. Sarapa, "International Use of X80: the Experience Base," ed. L. Fletcher *X80 Pipeline Cost Workshop*, (Hobart, AU: Australian Pipeline Industry Association Research and Standards Committee, 30 October 2002), 23-34.
2. S. Bremer et al., "HIPERC-A Novel, High Performance, Economic Steel Concept for Line Pipe and General Structural Use" (Research Fund for Coal and Steel, Final Report, 2009).
3. V. Flaxa and F.M. Knoop, "Characterization of Hot-rolled Strips of up to 18.9 mm in Thickness and their Processing to Helically Welded Large Diameter Pipes of Grade X80," *Proceedings of Pipeline Technology Conference 2009*, Ostend, Belgium, (2009), paper number 16.
4. S. Bremer, V. Flaxa and F.M. Knoop, "A Novel Alloying Concept for Thermo-Mechanical Hot-Rolled Strip for Large Diameter HTS (Helical Two Step) Line Pipe," *Proceedings of 7<sup>th</sup> International Pipeline Conference 2008*, Calgary, Canada, (2008), paper number IPC2008-64678.
5. S. Zimmermann et al., "Mechanical Properties and Component Behaviour of X80 Helical Seam Welded Large Diameter Pipes," *Proceedings of 8<sup>th</sup> International Pipeline Conference 2010*, Calgary, Canada, (2010), paper number IPC2010-31602.
6. S. Bremer, M. Masimov, B. Ouaisa, "Substructure and Texture-Related Anisotropy of Mechanical Properties of High Strength Bainitic X80 Steel for Spiral-Welded Pipe," *Proceedings of 2nd International Conference Super-High Strength Steels 2010*, Peschiera del Garda, Italy, (2010), paper number 38.
7. R.K. Ray and J.J. Jonas, "Transformation Textures in Steels," *International Materials Reviews*, 35 (1990), 1-36.
8. F.M. Knoop, C. Boppert and W. Schmidt, "Perfecting the Two-Step," *World Pipelines*, (March 2008), 29-38.
9. C. Holste and F.M. Knoop, Patent DE 10 2009 051 695 B3.
10. G. Knauf, G. Hohl and F.M. Knoop, "The Effect of Specimen Type on Tensile Test Result and its Implications for Line Pipe," *3R International* 40 (10-11/2001), 655-661.

11. E. Muthmann et al., "Large Diameter Induction Bends in Material Grade X80 Fabricated from TMCP Material," *Proceedings of Pipeline Technology Conference 2009*, Ostend, Belgium, (2009).
12. H. Motohashi, N. Hagiwara and T. Masuda, "Tensile Properties and Microstructure of Weld Metal of X80 Line Pipe Steel," (London, UK: International Institute of Welding), IIW Document XI-822-04.
13. K. Choong-Myeong, L. Jong-Bong and Y. Jang-Yong, "A Study on the Metallurgical and Mechanical Characteristics of the Weld Joint of X80 Steel," (Technical Research Laboratories, POSCO Pohang, Kyungbuk, Korea).
14. Standard EN 1011: Welding – Recommendations for welding of metallic materials – Part 2: Arc Welding of ferritic steels, German version.
15. J. Krampen, W. Scheller and M. Liedtke, "Welding Recommendations for Modern Tubular Steels," *Proceedings of 12<sup>th</sup> International Symposium on Tubular Structures 2008*, Shanghai, China, (2008).